Structural Insights into RNA Recognition Properties of Glyceraldehyde-3-phosphate Dehydrogenase 3 from Saccharomyces cerevisiae

ARTICLE *in* INTERNATIONAL UNION OF BIOCHEMISTRY AND MOLECULAR BIOLOGY LIFE · SEPTEMBER 2014

Impact Factor: 3.14 · DOI: 10.1002/iub.1313

6 AUTHORS, INCLUDING:

Liu Qiao
University of Science and Technology of China
3 PUBLICATIONS **20** CITATIONS
SEE PROFILE

Maikun Teng
University of Science and Technology of China
138 PUBLICATIONS **1,546** CITATIONS
SEE PROFILE

Xu Li
University of Science and Technology of China
58 PUBLICATIONS **379** CITATIONS
SEE PROFILE

Research Communication

Structural Insights into RNA Recognition Properties of Glyceraldehyde-3-phosphate Dehydrogenase 3 from *Saccharomyces cerevisiae*

Hui Shen[#]
Hong Wang[#]
Qiao Liu
Huihui Liu
Maikun Teng*
Xu Li*

School of Life Sciences, University of Science and Technology of China, Hefei, Anhui, People's Republic of China

Abstract

Glyceraldehyde-3-phosphate dehydrogenase (GAPDH, EC: 1.2.1.12) is an essential enzyme in the glycolytic pathway. However, recent evidence demonstrates that GAPDH displays a range of new functions unrelated to its glycolytic function. GAPDH has long been known as a 3′ AU-rich element-binding protein; however, its RNA recognition mechanism is still not well understood. Here, we present the first crystal structure of GAPDH3 from *Saccharomyces cerevisiae* and identify its RNA-binding specificity and propose an RNA recognition model based on structural and biochemical studies. This study sheds light on the RNA-binding mechanism of GAPDH3 and contributes to a better understanding of the molecular mechanisms of its RNA-related functions. © 2014 IUBMB Life, 00(00):000–000, 2014

Keywords: *GAPDH3; crystal structure; RNA binding; sequence specificity; RNA recognition model*

Introduction

Glyceraldehyde-3-phosphate dehydrogenase (GAPDH, EC: 1.2.1.12) has long been recognized as an important enzyme for energy metabolism and the production of ATP and pyruvate through anaerobic glycolysis in the cytoplasm (1). GAPDH also plays an important role in glycolysis and gluconeogenesis. It catalyses the oxidative phosphorylation of glyceraldehyde-3-phosphate (GAP) to 1,3-bisphosphoglycerate (BPG) in the presence of the cofactor nicotinamide adenine dinucleotide (NAD^+), which is the sixth reaction step of glycolysis (2). GAPDH commonly consists of a single polypeptide chain of ~335 amino acids (3). Each GAPDH monomer contains two binding domains: an N-terminal NAD^+-binding domain and a C-terminal catalytic, or glyceraldehyde-3-phosphate (G3P)-binding, domain (4). The glycolytic function relies on critical amino acids, including Cys^{152} and His^{179}, and on its tetrameric structure composed of four identical subunits (5).

Recently, a number of studies have indicated that GAPDH is not merely a simple glycolytic protein but rather has multiple roles in DNA replication and repair, apoptosis initiation, localization at the cell surface, binding to cellular molecules, membrane fusion and transport, tRNA export, and mRNA stability regulation (1, 6). As such, the study of GAPDH may be of importance not only in and of itself but also as a means to understand the relationship between protein structure and functional diversity (7).

GAPDH has long been known as a 3′ ARE-binding protein because it can selectively bind to AU-rich element (ARE; ref.

Abbreviations: *GAPDH, glyceraldehyde-3-phosphate dehydrogenase; GAPDH3, glyceraldehyde-3-phosphate dehydrogenase 3 from* ***Saccharomyces cerevisiae****; ARE, AU-rich element; FPA, fluorescence polarization assays; NAD^+, nicotinamide adenine dinucleotide; GAP, glyceraldehyde-3-phosphate; BPG, 1,3-bisphosphoglycerate; RMSD, root-mean-square deviation*

Volume 00, Number 00, Month 2014, Pages 00–00

[#]The first two authors are the joint first authors.

**Address for correspondence to: Xu Li, School of Life Sciences, University of Science and Technology of China, Hefei, Anhui 230026, China. Tel: +86-0551-63607334. Fax: +86-551-63607334. E-mail: sachem@ustc.edu.cn. or MaiKun Teng, School of Life Sciences, University of Science and Technology of China, Hefei, Anhui 230026, China. Tel: +86-0551-63606314. Fax: +86-551-63606314. E-mail: mkteng@ustc.edu.cn.*

Received 18 August 2014; Accepted 8 September 2014

DOI 10.1002/iub.1313

Published online 00 Month 2014 in Wiley Online Library (wileyonlinelibrary.com)

2). However, the RNA recognition mechanism of GAPDH is still not well understood. In the *Saccharomyces cerevisiae* genome, there are three unlinked GAPDH structural genes (*TDH1–3*) that encode closely related but not identical GAPDH isoforms (GAPDH1, GAPDH2, and GAPDH3, with sequence identities >90%; ref. *8*). The strains lacking one of the individual *TDH* genes can grow, but at lower rates than wild-type cells. However, the double-deletion mutant for *TDH2* and *TDH3* appears to be unviable (9). Previous research found that only the most basic isoform GAPDH1 has ARE-binding capacity (10). Nevertheless, our fluorescence polarization assays (FPAs) verified that the less common isoform GAPDH3 could also bind an AU-rich element. To investigate the RNA recognition mechanism of GAPDH3, we determined the 2.49 Å resolution structure of the apo-form of GAPDH3. The structural analysis and the protein–RNA interaction assays demonstrate its RNA-binding specificity, and we propose a RNA recognition model of GAPDH3.

Materials and Methods

Cloning, Expression, and Purification

Cloning, expression, and purification of full-length GAPDH3 from *S. cerevisiae* were described in our previous publication (11).

Crystallization, Data Collection, Structure Determination, and Model Refinement

The crystals of apo-form GAPDH3 were obtained at 287 K by vapor-diffusing 10 mg/mL protein against a reservoir of 12% (w/v) PEG3350, 0.1 M sodium malonate pH 4.0 after 2 days. Crystals were harvested using cryoloops and were first flash-frozen in liquid nitrogen with a cryoprotectant solution consisting of the reservoir solution supplemented with 20% glycerol and then transferred to the liquid nitrogen stream. The data for apo-GAPDH3 were collected at 100 K using a Jupiter CCD detector on the BL17U1 beamline at the Shanghai Synchrotron Radiation Facility. Diffraction data were integrated and scaled using HKL2000 software (12). The crystals belong to space group $I4_122$, with one molecule in the asymmetric unit and with unit cell dimensions: $a = b = 116.13$ Å and $c = 119.18$ Å. The Matthews coefficient is 2.87 Å^3/Da, with a solvent content of 57.18%. The structure was solved by the molecular replacement method with the MOLREP program (13) in the CCP4 package (14) using the crystal structure of *Escherichia coli* G3P1 in complex with NAD (identity 68%, Protein Data Bank [PDB] code: 1GAD; ref. *15*) as the search model. Refinement was performed by REFMAC5 (16). Between each round of refinement, the model was fit to the $2F_o - F_c$ electron-density map using the program COOT (17). The final refined model has an R (R_{free}) factor of 21.4% (27.4%). The quality of final model was checked with PROCHECK (18). The final detailed refinement statistics are summarized in Table 1. The coordinates and structure factors were deposited into the PDB with the accession code 4IQ8. Figures were prepared using PyMOL (DeLano Scientific LLC).

Enzymatic Activity Assays

GAPDH catalyses the oxidative phosphorylation of GAP to BPG in the presence of inorganic phosphate (Pi) and NAD^+, and its activity can be monitored by measuring the formation of nicotinamide adenine dinucleotide hydrogen. Enzymatic activity assays were performed using a DU800 spectrophotometer (Beckman Coulter) at 298 K according to the published method (19). In a 300 μL reaction mix (40 mM triethanolamine, 50 mM Na_2HPO_4, and 5 mM EDTA, pH 8.6), the concentration of NAD^+ was varied while maintaining the GAP substrate at a fixed saturating level. The change in absorbance in first 20 sec at 340 nm was monitored. All values were the average of three measurements.

Fluorescence Polarization Assays

The sequences of the fluorescently labeled (5′-FAM) RNA probes are AUUUAUUUAUUUA, AUUUAUUUA, AUUUA, poly(A)$_{13}$, poly(U)$_{13}$, and poly(C)$_{13}$ (Takara). FPAs were performed in Tris-HCl buffer (20 mM Tris pH 8.0, 200 mM NaCl) at 293 K using a SpectraMax M5 microplate reader system. The wavelengths of fluorescence excitation and emission were 490 and 522 nm, respectively. Each well of a 384-well plate contained an 80 nM 5′-FAM RNA probe and different concentrations of GAPDH3 alone or GAPDH3 mixed with NAD^+ at a final volume of 80 μL. For each assay, RNA-free controls were included. The fluorescence polarization P (in mP units) was calculated as follows:

$$P = (I// - I\perp)/(I// + I\perp). \quad (1)$$

The fluorescence polarization change ΔP (in mP units) was fitted into the following equation:

$$\Delta P = \Delta P_{max} \times \{[protein]/(K_d + [protein])\} \quad (2)$$

The binding curves were fit using ORIGIN software (http://www.originlab.com), and error bars were derived from three independent assays.

Results and Discussion

RNA Recognition Properties of GAPDH3

Enzymatic activity studies of recombinant *S. cerevisiae* GAPDH3 showed that the apparent K_{NAD} is ~686 μM (Fig. 1A), which is close to the value reported for homologous GAPDHs (19). This result indicated that the recombinant GAPDH3 was correctly folded and had biological activity.

As mentioned above, GAPDH usually has AU-rich mRNA-binding capabilities. Karpel and Burchard (10) reported that of the three isoforms in *S. cerevisiae*, only the basic GAPDH1 isoform has ARE-binding capacity. To investigate whether the less basic GAPDH3 isoform from *S. cerevisiae* could bind to AU-rich mRNA, we performed a FPA. An mRNA sequence containing three iterations of AUUUA (13-base AUUUAUUUAUUUA, termed as 3*AUUUA) was selected for FPA. As shown in Fig. 1B, GAPDH3 bound to the 13-base

TABLE 1 *Data collection statistics and refinement statistics*

Data collection	
Space group	$I4_122$
Unit cell (Å)	$a = b = 116.13$, $c = 119.18$
Wavelength (Å)	0.9792
Resolution (Å)[a]	50–2.49 (2.53–2.49)
Unique reflections	14,571
Completeness (%)	99.7 (100.0)
I/σ (I)	40.8 (7.7)
R_{merge} (%)[b]	6.4 (45.9)
Redundancy	10.5 (10.8)
Refinement statistics	
R_{work}/R_{free} (%)	21.4/27.4
Number of water molecules	20
RMSD bond length (Å)	0.010
RMSD bond angle (°)	1.182
Average B-factors (Å^2)	50.2
PDB code	4IQ8

[a] *Values in parenthesis are for the highest resolution shell.*
[b] $R_{merge} = \Sigma_{hkl}\Sigma_i |I_i(hkl) - <I(hkl)>| / \Sigma_{hkl}\Sigma_i I_i(hkl)$, *where* Σ_{hkl} *is the sum over all reflections and* Σ_i *is the sum over all equivalent and symmetry-related reflections.*

AU-rich segment with a K_d of 110.91 ± 12.64 μM. The FPA result indicates that GAPDH3 also has RNA-binding ability *in vitro*.

To investigate the RNA-binding specificity of GAPDH3, we performed FPAs for GAPDH3 with 13-base poly(A)$_{13}$, poly(U)$_{13}$, and poly(C)$_{13}$ segments. There was no obvious GAPDH3 binding capacity for poly(C)$_{13}$, and only at high concentrations (>200 mM) could GAPDH3 bind poly(U)$_{13}$ with a very small binding affinity. However, poly(A)$_{13}$ showed a similar binding affinity to that of 3*AUUUA with a K_d value of 154.44 ± 26.94 μM (Fig. 1B). The data above indicated that GAPDH3 in *S. cerevisiae* has sequence-specific recognition for AU-rich or polyadenosine RNA substrates but not for the polycytidine or polyuridine RNA substrates.

Crystal Structure of Apo-Form GAPDH3

To investigate the interaction mechanism between GAPDH3 and ARE substrates, we attempted to solve the structures of GAPDH3 complexed with different length AU-rich RNA [AUUUAUUUAUUUA, AUUUAUUUA, AUUUA, and poly(A)$_{13}$]. Unfortunately, we did not obtain any diffraction-quality crystals of the protein:RNA complex. In the end, we determined the apo-form GAPDH3 crystal structure at 2.49 Å resolution in space group $I4_122$.

In the structure of *S. cerevisiae* GAPDH3, each asymmetric unit contains one molecule. Similar to other structures of GAPDH, it is composed of two domains: the NAD^+-binding domain (residues 1–149) and the catalytic domain (residues 150–332; Fig. 2A). The NAD^+-binding domain has a classical dinucleotide binding fold—the Rossmann fold (20). This domain contains eight β-sheets in which these strands are interconnected by either short loops or helices. There are also four helices in this domain. The catalytic domain consists of eight mixed β-strands and three long α-helices, in which α1

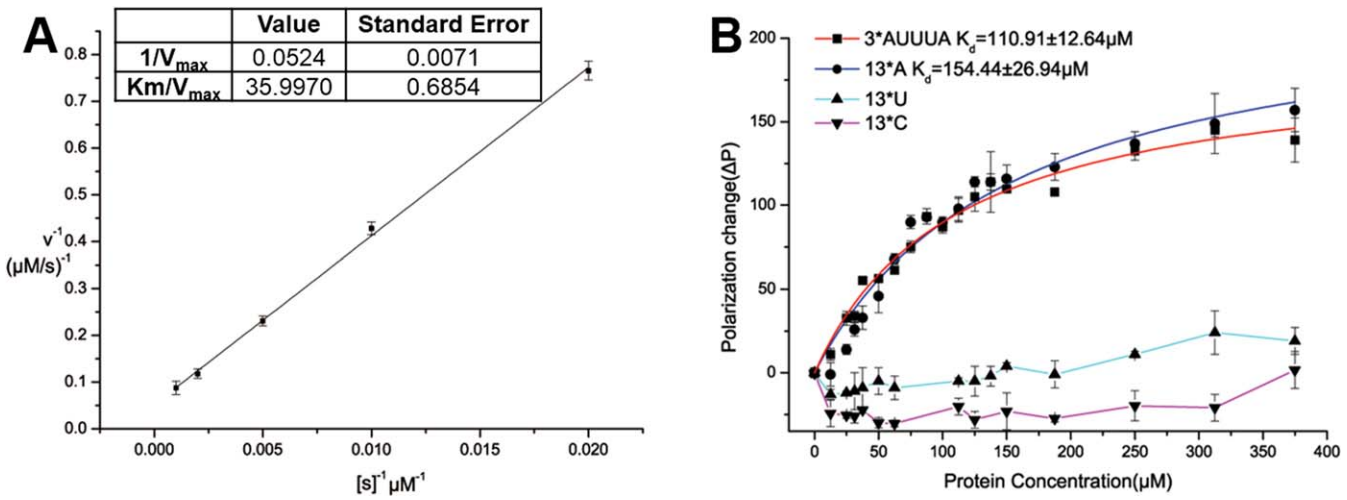

FIG 1 *A: The enzymatic activity curve of GAPDH3. B: The 13-base AU-rich and poly(A)$_{13}$, poly(U)$_{13}$, and poly(C)$_{13}$ oligo binding curves of GAPDH3 by FPA. [Color figure can be viewed in the online issue, which is available at wileyonlinelibrary.com.]*

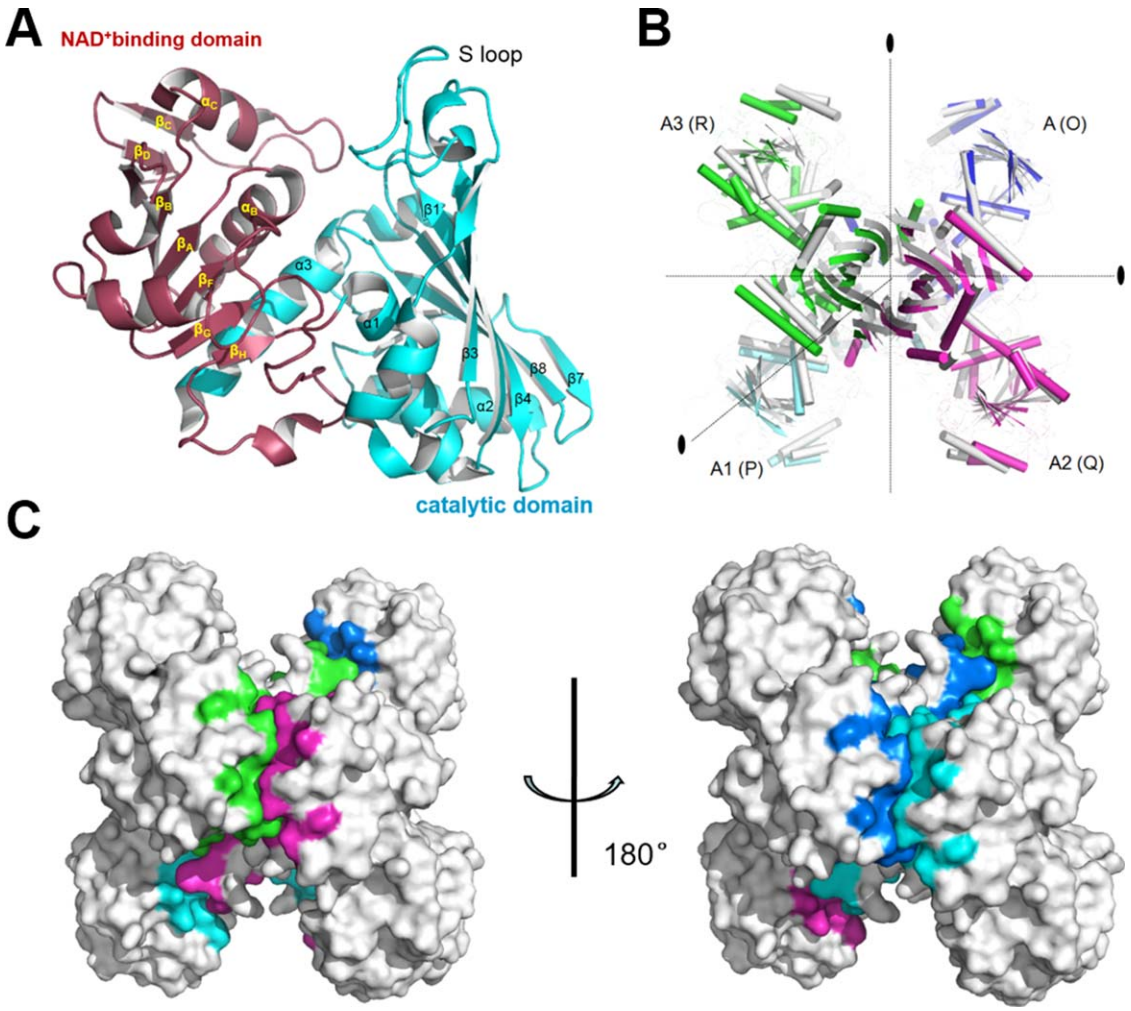

FIG 2

A: Overall structure of S. cerevisiae *GAPDH3. The NAD$^+$-binding domain and catalytic domain are colored ruby and cyan, respectively. B: Spatial organization of the tetramer obtained by comparison with one homologous structure (gray, PDB code: 3LVF) and operating through three crystallographic twofold axes. The subunits A (blue), A1 (cyan), A2 (magenta), and A3 (green) correspond to the subunits O, P, Q, and R, respectively, of the homologous structure (PDB code: 3LVF). C: Schematic view of the tetramer contact surface. The interacting areas on each GAPDH3 molecule are colored red, green, blue, and deep blue, respectively. [Color figure can be viewed in the online issue, which is available at wileyonlinelibrary.com.]*

links the NAD$^+$-binding domain and the catalytic domain and α3 fits into a groove of the NAD$^+$-binding domain. The relatively flexible S-loop (residues 178–205) in the catalytic domain is clearly visible in our structure, with high-quality electron density in this region.

Superimposition of the NAD$^+$-binding domain of GAPDH3 from *S. cerevisiae* with the O-subunit of GAPDH from *Staphylococcus aureus* (PDB code: 3LC7, sequence identity: 45%; ref. *21*) gives a root-mean-square difference (RMSD) of 0.68 Å for 147 C$^\alpha$ positions. Superimposition of the catalytic domains of these two structures shows an RMSD of 0.71 Å for 178 C$^\alpha$ position. The variations of the flexible loops result in insignificant differences between these two structures. However, the low RMSD values suggest that the overall structures of these two GAPDH are comparable with each other despite distinct difference in their sequences.

As is known, GAPDH exists as a homotetramer, homodimer, or monomer in the cell (22–24). The tetrameric form is located mainly in the cytoplasm and is composed of four identical subunits (25). The monomeric form is localized to the nucleus, mainly during cell proliferation (26). To identify the oligomerization state of recombinant *S. cerevisiae* GAPDH3, a size exclusion chromatography (SEC) assay was carried out. The SEC assay showed that *S. cerevisiae* GAPDH3 exists as a tetramer in solution (11). Although the asymmetric unit of the *S. cerevisiae* GAPDH3 structure contains only one unit, analysis by PISA indicates that the most probable assembly of the protein is tetramer (27). In each tetramer, the surface areas at the interface of one monomer binding to the neighboring three are 1881.1 Å, 1302.1 Å, and 492.2 Å, which occupy more than a quarter of the total surface area of each monomer (14,694 Å; Fig. 2C). The data suggest that the tetramer state of

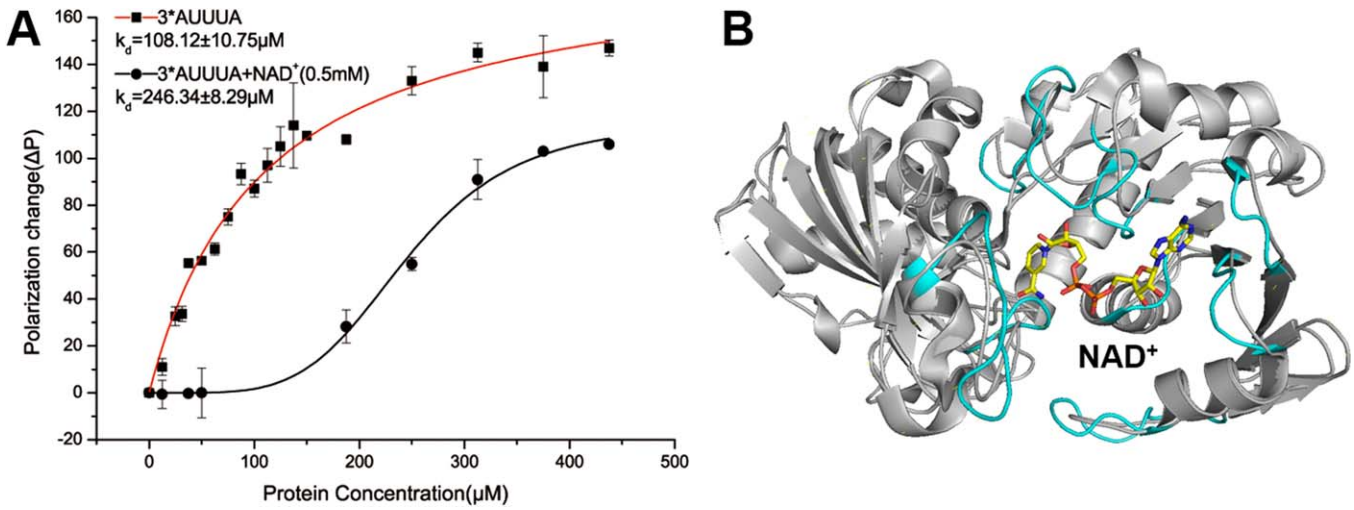

FIG 3

A: The NAD$^+$ inhibition analysis for the 13-base AU-rich substrate by FPA. GAPDH3 (red) and GAPDH3 mixed with 0.5 mM NAD$^+$ (black) bind to the 13-base AU-rich mRNA with K_d values of 108.12 ± 10.75 μM and 246.34 ± 8.29 μM, respectively. B: NAD$^+$ binding only induces tiny structural changes in the local environment close to the NAD$^+$-binding pocket on NAD$^+$ binding. The loops, which are near the NAD$^+$-binding pocket, assemble to the NAD$^+$ molecule on NAD$^+$ binding (cyan loops). [Color figure can be viewed in the online issue, which is available at wileyonlinelibrary.com.]

GAPDH3 exists and is stable in solution. The tetrameric state of GAPDH3 was confirmed by comparisons with homologous structures and by crystallographic symmetry after examining three crystallographic twofold axes (Fig. 2B).

The NAD$^+$ Inhibition of GAPDH3 RNA-Binding Capability

Because it has been reported that incubation of GAPDH with its cofactor NAD$^+$ reduces its interaction with tRNA (28), viral RNA (29), and interferon-ARE (2), we were interested in whether NAD$^+$ also affected the RNA-binding capability of GAPDH3. We added 0.5 mM NAD$^+$ into the FPA reaction systems, and GAPDH3 bound to the 13-base AU-rich RNA oligo with a K_d value of 246.34 ± 8.29 μM using the Langmuir-Hill equation, with a Hill coefficient of 4.7 (Fig. 3A). As the interaction curve reached saturation, the binding strength between GAPDH3 and the AU-rich oligo with NAD$^+$ (polarization change ΔP was ~100) was still 33% less than that without NAD$^+$ (polarization change ΔP was ~150; Fig. 3A). These results indicated that NAD$^+$ could inhibit the RNA-binding capability of GAPDH3. The high Hill coefficient also revealed the existence of positively cooperative binding and indicated that the RNA substrate binding to GAPDH3 tetramer facilitates NAD$^+$ release and enables new RNA substrate to bind to GAPDH3.

There were two possible mechanisms of the NAD$^+$ inhibition for GAPDH3 RNA-binding capability. The first was that NAD$^+$ binding could induce significant conformational changes in GAPDH3 and decrease its affinity for binding to RNA. The second was that GAPDH3 could bind to AU-rich mRNA through its NAD$^+$-binding domain, and thus, NAD$^+$ binding could block the RNA-binding site of GAPDH3.

Recently, the PDB released the structure of *S. cerevisiae* GAPDH3 in complex with NAD$^+$ (PDB code: 3PYM). The asymmetric unit of the complex structure comprises two molecules. Superposition of chains A and B results in an RMSD of 0.157 Å, indicating that there are no dramatic differences between the two subunits. Therefore, we describe one such subunit in the asymmetric unit here. A superposition between our apo-form structure and this complex structure shows that the binding of NAD$^+$ only causes the loops near the NAD$^+$-binding pocket to assemble to the NAD$^+$ molecule but does not change the overall conformation of GAPDH3 (Fig. 3B), and the catalytic domain remains unaffected. The two NAD$^+$-binding domains superimpose with an RMSD of 0.27 Å, whereas the catalytic domains superimpose with an RMSD of 0.18 Å. The structural comparison between the apo-form and the NAD$^+$-binding form GAPDH3 indicated that NAD$^+$ binding does not induce prominent conformational changes in GAPDH3, which could decrease the affinity of GAPDH3 binding to RNA. Rather, the above data about the NAD$^+$ inhibition for GAPDH3 RNA binding capability indicated that GAPDH3 likely binds to the AU-rich or polyadenosine RNA substrates through its NAD$^+$-binding domain *in vitro*.

The RNA Recognition Model of GAPDH3

As mentioned above, GAPDH3 exists as a tetramer in solution. By analyzing the surface electrostatic potential, we found that there were two consecutive positively charged regions that contained an NAD$^+$-binding site, one of which was located on each side of the tetramer (Fig. 4A). Combined with our structural analysis and FPA results, we hypothesized that these two positively charged grooves could be the RNA-binding sites of the GAPDH3 tetramer; one GAPDH3 tetramer could bind two separate RNA strands or two separate AREs in a single RNA strand.

Because the length of each positively charged RNA-binding groove was ~56 Å, consistent with an ~16-nt RNA strand, we

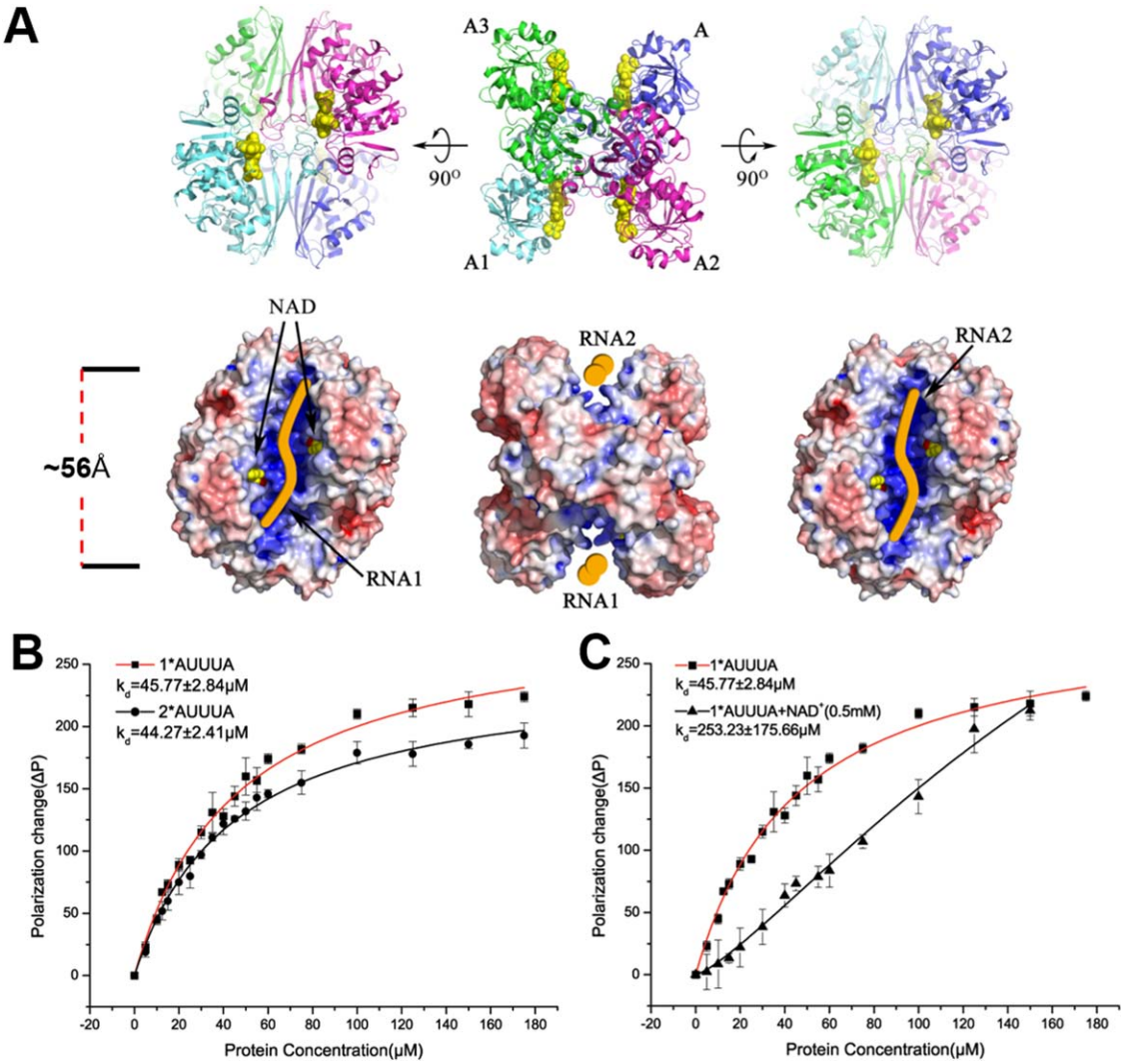

FIG 4

A: Model of the GAPDH3 homotetramer complexed with RNA. A yellow ball denotes NAD^+. A golden rod denotes the RNA molecule. Four subunits of GAPDH3 are colored blue, cyan, magenta, and green, respectively. B: The 9-base (black) and 5-base (red) AU-rich oligo binding curves of GAPDH3 by FPA. C: The NAD^+ inhibition analysis for the 5-base AU-rich substrate by FPA. GAPDH3 (red) and GAPDH3 mixed with 0.5 mM NAD^+ (black) bind to the 5-base AU-rich mRNA with K_d values of 45.77 ± 2.84 μM and 253.23 ± 175.66 μM, respectively. [Color figure can be viewed in the online issue, which is available at wileyonlinelibrary.com.]

focused that whether the length of the RNA substrate affected the binding affinity of GAPDH3. The FPAs between GAPDH3 and different length AU-rich RNAs (9-base AUUUAUUUA, termed as 2*AUUUA; and 5-base AUUUA, termed as 1*AUUUA) were performed. The results indicated that GAPDH3 bound 1*AUUUA and 2*AUUUA with similar K_d values of 45.77 ± 2.84 μM and 44.27 ± 2.41 μM, respectively, which were both higher than that of 3*AUUUA (Fig. 4B). It indicated that the positively charged RNA-binding groove was inclined to recognize a single iteration of the AUUUA sequence, and thus, GAPDH3 showed almost the same affinity for the 1*AUUUA as the 2*AUUUA substrate.

An NAD^+ inhibition test with the 1*AUUUA substrate was also performed by FPA. When 0.5 mM NAD^+ was added into reaction system, GAPDH3 bound to the 5-base AUUUA oligo with a K_d value of 253.23 ± 175.66 μM using the Langmuir-Hill equation, with a Hill coefficient of 1.3 (Fig. 4C). This indicated that NAD^+ could inhibit the AUUUA-binding capacity of GAPDH3; however, the inhibition effect was weaker for the 5-base substrate than for the 13-base substrate. If the GAPDH3 concentration was above 0.15 mM, this inhibition effect almost disappeared. We hypothesized that it was because of one positively charged groove containing two NAD^+-binding sites; when 0.5 mM NAD^+ was added into the reaction system, two NAD^+-binding sites of GAPDH3 were occupied. RNA substrate binding needed to competitively displace the NAD^+ molecules from the binding groove. The 5-base AUUUA binding only needed to displace one NAD^+ molecule; however, the 13-base

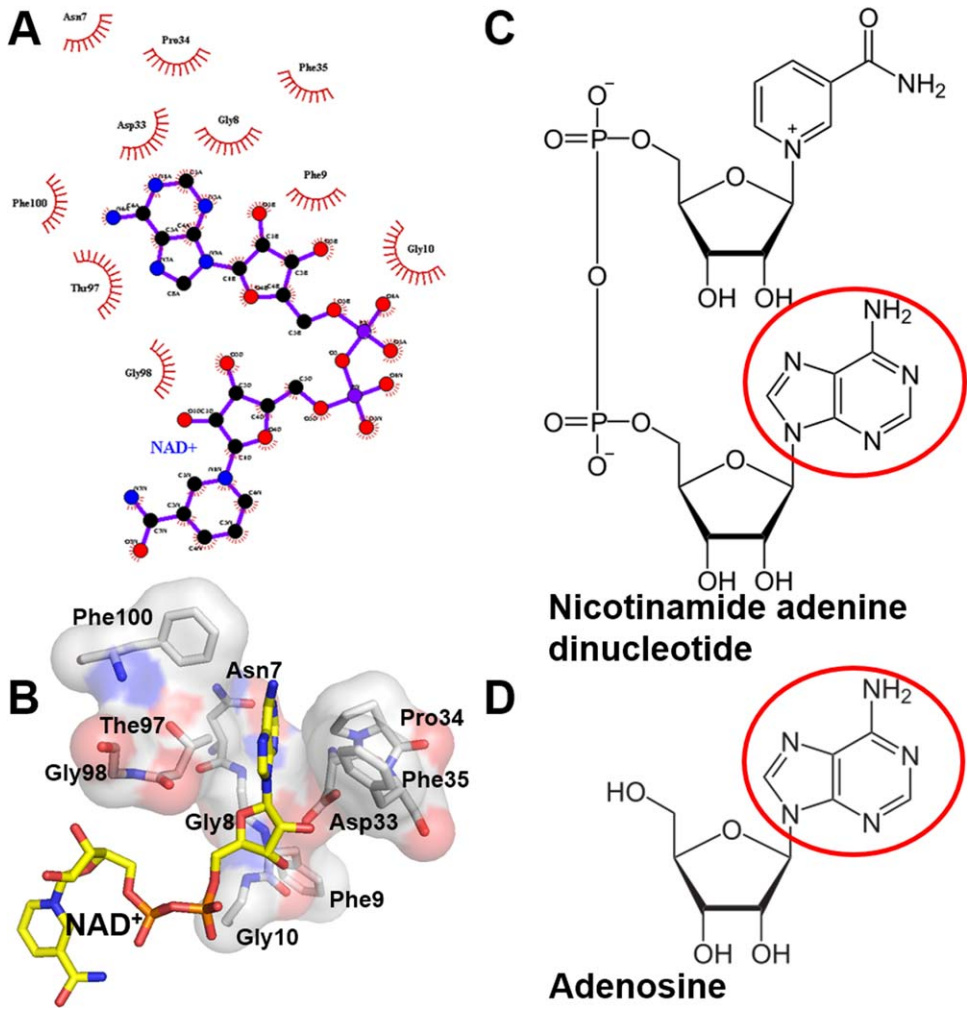

FIG 5

A: The protein–NAD$^+$ contacts of GAPDH3. Residues Asn^7, Gly^8, Phe^9, Gly^{10}, Asp^{33}, Pro^{34}, Phe^{35}, The^{97}, Gly^{98}, and Phe^{100} tightly enclose the pyrimidine ring of NAD$^+$ by hydrophobic interactions. B: The NAD$^+$ molecule inserts a pyrimidine ring into a narrow hydrophobic binding pocket on the positively charged surface of GAPDH3. Skeletal formula of (C) nicotinamide adenine dinucleotide and (D) adenosine. [Color figure can be viewed in the online issue, which is available at wileyonlinelibrary.com.]

3*AUUUA binding needed to displace two NAD$^+$ molecules. Therefore, even though NAD$^+$ was present, the affinity of the 13-base 3*AUUUA substrate for GAPDH3 was much lower than that of the 5-base AUUUA at the same GAPDH3 concentration.

Furthermore, by structural analysis, we found that the NAD$^+$ molecule inserted its pyrimidine ring into a narrow hydrophobic binding pocket on the positively charged surface of GAPDH3 (Fig. 5B). The residues Asn^7, Gly^8, Phe^9, Gly^{10}, Asp^{33}, Pro^{34}, Phe^{35}, The^{97}, Gly^{98}, and Phe^{100} tightly enclosed the pyrimidine ring of NAD$^+$ (Figs. 5A and 5B). Because of a common adenine head, adenosine can also bind tightly to this hydrophobic binding pocket (Figs. 5C and 5D). Because the amidogen on the adenine ring π-conjugates to the six-membered ring, the chemical polarity of the adenine is much lower than that of guanine, cytosine, and uracil. Guanosine, cytidine, and uridine bind to the hydrophobic binding pocket with lower affinity than that of adenosine. Based on these discoveries, we speculated that the sequence-specific recognition of GAPDH3 comes from the tight binding of adenosine to the two hydrophobic pyrimidine ring binding pocket on the positively charged grooves. The other regions on the positively charged groove only provide a nonspecific binding surface for the RNA substrate. Although this hypothesis is consistent with all of our data, further experimental evidence is needed to confirm it.

Acknowledgements

The authors thank the staff at Shanghai Synchrotron Radiation Facility beamline BL17U for assistance with synchrotron data collection. The authors declare no conflict of interest. Financial support for this project was provided by the Chinese National Natural Science Foundation (Grant No. 31130018), the Chinese Ministry of Science and Technology (Grant No. 2012CB917200), the Chinese National Natural Science

Foundation (Grant Nos. 31370732 and 31270014), and the Science and Technological Fund of Anhui Province for Outstanding Youth (Grant No. 1308085JGD08).

References

[1] Nicholls, C., Li, H., and Liu, J. P. (2012) GAPDH: a common enzyme with uncommon functions. Clin. Exp. Pharmacol. Physiol. 39, 674–679.

[2] Nagy, E., and Rigby, W. F. C. (1995) Glyceraldehyde-3-phosphate dehydrogenase selectively binds Au-rich RNA in the Nad(+)-binding region (Rossmann Fold). J. Biol. Chem. 270, 2755–2763.

[3] Colell, A., Green, D. R., and Ricci, J. E. (2009) Novel roles for GAPDH in cell death and carcinogenesis. Cell Death Differ. 16, 1573–1581.

[4] Jenkins, J. L., and Tanner, J. J. (2006) High-resolution structure of human D-glyceraldehyde-3-phosphate dehydrogenase. Acta Crystallogr. D Biol. Crystallogr. 62, 290–301.

[5] Sirover, M. A. (1999) New insights into an old protein: the functional diversity of mammalian glyceraldehyde-3-phosphate dehydrogenase. Biochim. Biophys. Acta 1432, 159–184.

[6] Zhou, Y., Yi, X., Stoffer, J. B., Bonafe, N., Gilmore-Hebert, M., et al. (2008) The multifunctional protein glyceraldehyde-3-phosphate dehydrogenase is both regulated and controls colony-stimulating factor-1 messenger RNA stability in ovarian cancer. Mol. Cancer Res. 6, 1375–1384.

[7] Sirover, M. A. (2012) Subcellular dynamics of multifunctional protein regulation: mechanisms of GAPDH intracellular translocation. J. Cell. Biochem. 113, 2193–2200.

[8] Delgado, M. L., O'Connor, J. E., Azorin, I., Renau-Piqueras, J., Gil, M. L., et al. (2001) The glyceraldehyde-3-phosphate dehydrogenase polypeptides encoded by the *Saccharomyces cerevisiae* TDH1, TDH2 and TDH3 genes are also cell wall proteins. Microbiology 147, 411–417.

[9] McAlister, L., and Holland, M. J. (1985) Isolation and characterization of yeast strains carrying mutations in the glyceraldehyde-3-phosphate dehydrogenase genes. J. Biol. Chem. 260, 15013–15018.

[10] Karpel, R. L., and Burchard, A. C. (1981) A basic isozyme of yeast glyceraldehyde-3-phosphate dehydrogenase with nucleic acid helix-destabilizing activity. Biochim. Biophys. Acta 654, 256–267.

[11] Liu, Q., Wang, H., Liu, H., Teng, M., and Li, X. (2012) Preliminary crystallographic analysis of glyceraldehyde-3-phosphate dehydrogenase 3 from *Saccharomyces cerevisiae*. Acta Crystallogr. Sect. F Struct. Biol. Cryst. Commun. 68, 978–980.

[12] Otwinowski, Z., and Minor, W. (1997) Processing of X-ray diffraction data collected in oscillation mode. Macromol. Crystallogr. A 276, 307–326.

[13] Vagin, A., and Teplyakov, A. (1997) MOLREP: an automated program for molecular replacement. J. Appl. Crystallogr. 30, 1022–1025.

[14] Bailey, S. (1994) The Ccp4 suite—programs for protein crystallography. Acta Crystallogr. D 50, 760–763.

[15] Duee, E., Olivier-Deyris, L., Fanchon, E., Corbier, C., Branlant, G., et al. (1996) Comparison of the structures of wild-type and a N313T mutant of *Escherichia coli* glyceraldehyde 3-phosphate dehydrogenases: implication for NAD binding and cooperativity. J. Mol. Biol. 257, 814–838.

[16] Murshudov, G. N., Vagin, A. A., and Dodson, E. J. (1997) Refinement of macromolecular structures by the maximum-likelihood method. Acta Crystallogr. D 53, 240–255.

[17] Emsley, P., and Cowtan, K. (2004) Coot: model-building tools for molecular graphics. Acta Crystallogr. Sect. D: Biol. Crystallogr. 60, 2126–2132.

[18] Laskowski, R. A., Rullmann, J. A. C., MacArthur, M. W., Kaptein, R., and Thornton, J. M. (1996) AQUA and PROCHECK-NMR: programs for checking the quality of protein structures solved by NMR. J. Biomol. NMR 8, 477–486.

[19] Modun, B., and Williams, P. (1999) The staphylococcal transferrin-binding protein is a cell wall glyceraldehyde-3-phosphate dehydrogenase. Infect. Immun. 67, 1086–1092.

[20] Rao, S. T., and Rossmann, M. G. (1973) Comparison of super-secondary structures in proteins. J. Mol. Biol. 76, 241–256.

[21] Mukherjee, S., Dutta, D., Saha, B., and Das, A. K. (2010) Crystal structure of glyceraldehyde-3-phosphate dehydrogenase 1 from methicillin-resistant *Staphylococcus aureus* MRSA252 provides novel insights into substrate binding and catalytic mechanism. J. Mol. Biol. 401, 949–968.

[22] Engel, M., Seifert, M., Theisinger, B., Seyfert, U., and Welter, C. (1998) Glyceraldehyde-3-phosphate dehydrogenase and Nm23-H1/nucleoside diphosphate kinase A. Two old enzymes combine for the novel Nm23 protein phosphotransferase function. J. Biol. Chem. 273, 20058–20065.

[23] Roitel, O., Sergienko, E., and Branlant, G. (1999) Dimers generated from tetrameric phosphorylating glyceraldehyde-3-phosphate dehydrogenase from *Bacillus stearothermophilus* are inactive but exhibit cooperativity in NAD binding. Biochemistry 38, 16084–16091.

[24] Carlile, G. W., Chalmers-Redman, R. M., Tatton, N. A., Pong, A., Borden, K. E., et al. (2000) Reduced apoptosis after nerve growth factor and serum withdrawal: conversion of tetrameric glyceraldehyde-3-phosphate dehydrogenase to a dimer. Mol. Pharmacol. 57, 2–12.

[25] Roitel, O., Vachette, P., Azza, S., and Branlant, G. (2003) *P* but not *R*-axis interface is involved in cooperative binding of NAD on tetrameric phosphorylating glyceraldehyde-3-phosphate dehydrogenase from *Bacillus stearothermophilus*. J. Mol. Biol. 326, 1513–1522.

[26] Corbin, I. R., Gong, Y., Zhang, M., and Minuk, G. Y. (2002) Proliferative and nutritional dependent regulation of glyceraldehyde-3-phosphate dehydrogenase expression in the rat liver. Cell Prolif. 35, 173–182.

[27] Krissinel, E., and Henrick, K. (2007) Inference of macromolecular assemblies from crystalline state. J. Mol. Biol. 372, 774–797.

[28] Singh, R., and Green, M. R. (1993) Sequence-specific binding of transfer RNA by glyceraldehyde-3-phosphate dehydrogenase. Science 259, 365–368.

[29] Schultz, D. E., Hardin, C. C., and Lemon, S. M. (1996) Specific interaction of glyceraldehyde 3-phosphate dehydrogenase with the 5′-nontranslated RNA of hepatitis A virus. J. Biol. Chem. 271, 14134–14142.